# Uncoupling of the base excision and nucleotide incision repair pathways reveals their respective biological roles

**Alexander A. Ishchenko[†], Eric Deprez[‡§], Andrei Maksimenko[‡§¶], Jean-Claude Brochon[‡], Patrick Tauc[‡], and Murat K. Saparbaev[†‖]**

[†]Groupe Réparation de l'ADN, Unité Mixte de Recherche 8126, Centre National de la Recherche Scientifique, Institut Gustave Roussy, 94805 Villejuif Cedex, France; [‡]Laboratoire de Biotechnologie et Pharmacologie Génétique Appliquée, Unité Mixte de Recherche 8113, Centre National de la Recherche Scientifique, Ecole Normale Supérieure de Cachan, 94235 Cachan Cedex, France; and [¶]BioAlliance Pharma, 59, Boulevard du Général Martial Valin, 75015 Paris, France

Edited by Philip C. Hanawalt, Stanford University, Stanford, CA, and approved December 21, 2005 (received for review September 30, 2005)

**The multifunctional DNA repair enzymes apurinic/apyrimidinic (AP) endonucleases cleave DNA at AP sites and 3′-blocking moieties generated by DNA glycosylases in the base excision repair pathway. Alternatively, in the nucleotide incision repair (NIR) pathway, the same AP endonucleases incise DNA 5′ of a number of oxidatively damaged bases. At present, the physiological relevance of latter function remains unclear. Here, we report genetic dissection of AP endonuclease functions in base excision repair and NIR pathways. Three mutants of *Escherichia coli* endonuclease IV (Nfo), carrying amino acid substitutions H69A, H109A, and G149D have been isolated. All mutants were proficient in the AP endonuclease and 3′-repair diesterase activities but deficient in the NIR. Analysis of metal content reveals that all three mutant proteins have lost one of their intrinsic zinc atoms. Expression of the *nfo* mutants in a repair-deficient strain of *E. coli* complemented its hypersensitivity to alkylation but not to oxidative DNA damage. The differential drug sensitivity of the mutants suggests that the NIR pathway removes lethal DNA lesions generated by oxidizing agents. To address the physiological relevance of the NIR pathway in human cells, we used the fluorescence quenching mechanism of molecular beacons. We show that in living cells a major human AP endonuclease, Ape1, incises DNA containing α-anomeric 2′-deoxyadenosine, indicating that the intracellular environment supports NIR activity. Our data establish that NIR is a distinct and separable function of AP endonucleases essential for handling lethal oxidative DNA lesions.**

apurinic/apyrimidinic endonuclease | oxidative DNA damage | *tert*-butyl hydroperoxide | 3′-blocking groups | α-anomeric 2′-deoxyadenosine

Exogenous factors, such as ionizing radiation and chemical compounds, generate reactive oxygen species, such as $O_2^{\cdot-}$, $H_2O_2$, and OH·. DNA is one of the critical cellular targets for oxygen radicals. Reactive oxygen species produce mainly nonbulky DNA lesions that are substrates for two overlapping pathways: base excision repair (BER) and nucleotide incision repair (NIR). In the BER pathway a DNA glycosylase cleaves the *N*-glycosylic bond between the abnormal base and deoxyribose, leaving either an abasic site or a single-stranded break in DNA (1). Alternatively, in the NIR pathway, an apurinic/apyrimidinic (AP) endonuclease incises oxidatively damaged DNA in a DNA glycosylase-independent manner, providing the correct ends for DNA synthesis coupled to the repair of the remaining 5′-dangling modified nucleotide (2). Obviously, this latter mechanistic feature is distinct from DNA glycosylase-mediated BER. We have proposed that NIR participates *in vivo* in the removal of lethal oxidative DNA base damage (3). However, at present the physiological relevance of the NIR pathway remains unclear.

*Escherichia coli* has two AP endonucleases: exonuclease III (Xth) and endonuclease IV (Nfo). Nfo is an EDTA-resistant multifunctional enzyme with AP endonuclease, 3′-phosphatase and 3′-phosphoglycoaldehyde diesterase activities (4). The protein contains three $Zn^{2+}$ ions in the active site that are critical for its functions (5, 6). The *nfo* gene is under the control of the *soxRS* system and inducible by $O_2^{\cdot-}$ and NO· radicals (7). *E. coli nfo* mutants are hypersensitive to an anticancer drug, bleomycin, as well as to organic peroxide, *tert*-butyl-hydroperoxide (*t*-Bu$O_2$H), under conditions of chronic exposure to the drugs (8) and to macrophage generated NO· radicals (9). In addition, the double *nfo xth* mutants are more sensitive to γ-radiation, $H_2O_2$, and alkylating agents compared with *nfo* and *xth* single mutants. Thus, Nfo operates in both pathways: It repairs specific classes of oxidative damage and serves as a backup activity for Xth in repairing AP sites and 3′-blocking termini. Importantly, Nfo, but not Xth, is involved in the NIR pathway and is able to process a broad range of DNA lesions generated by oxidative stress, such as 5,6-dihydro-2′-deoxyuridine (DHU), 5,6-dihydrothymidine (DHT), 5-hydroxy-2′-deoxyuridine, 2,6-diamino-4-hydroxy-5-*N*-methylformamidopyrimidine, α-2′-deoxyadenosine (αA), and α-thymidine (2, 10, 11).

The NIR pathway is evolutionary conserved from *E. coli* and yeast to human cells, where the major AP endonuclease, Ape1/Ref-1/HAP-1 also incises duplex oligonucleotides containing DHU, αA, and α-thymidine residues (3). Previously, Ape1 was independently discovered as an abasic site-specific endonuclease homologous to the *E. coli* Xth protein (7) and as redox-regulator of the DNA-binding domain of Fos-Jun, Jun-Jun, AP-1 proteins, and several other transcription factors (12). Ape1 plays a central role in the short- and long-patch BER (13). Ape1 also exhibits other DNA repair activities: 3′→5′ exonuclease, phosphodiesterase, 3′-phosphatase, and RNase H (7). Based on the lack of a readily discernable phenotype of DNA glycosylase-deficient mice (14) and the increased susceptibility to oxidative stress of Ape1 heterozygous-null mutant mice (15), we proposed that the NIR function of Ape1 serves as a back-up pathway for BER. However pH, ionic strength, and divalent cation requirements of the Ape1-catalyzed NIR versus the AP endonuclease activities are dramatically different (3). In the present study, we attempted to address two critical questions: (*i*) to what extent NIR is an important function *in vivo* and (*ii*) whether NIR is a general property of AP endonucleases under intracellular conditions. The role of the AP endonuclease-initiated NIR pathway in counteracting oxidative stress is discussed.

---

Conflict of interest statement: No conflicts declared.

This paper was submitted directly (Track II) to the PNAS office.

Abbreviations: AP, apurinic/apyrimidinic; THF, tetrahydrofuran; DHU, 5,6-dihydro-2′-deoxyuridine; DHT, 5,6-dihydrothymidine; αA, α-2′-deoxyadenosine; NIR, nucleotide incision repair; BER, base excision repair; MMS, methylmethanesulfonate; *t*-Bu$O_2$H, *tert*-butyl hydroperoxide; PAR, 4-(2-pyridylazo)resorcinol; siRNA, small inhibitory RNA.

[§]E.D. and A.M. contributed equally to this work.

[‖]To whom correspondence should be addressed. E-mail: smurat@igr.fr.





www.pnas.org/cgi/doi/10.1073/pnas.0508582103

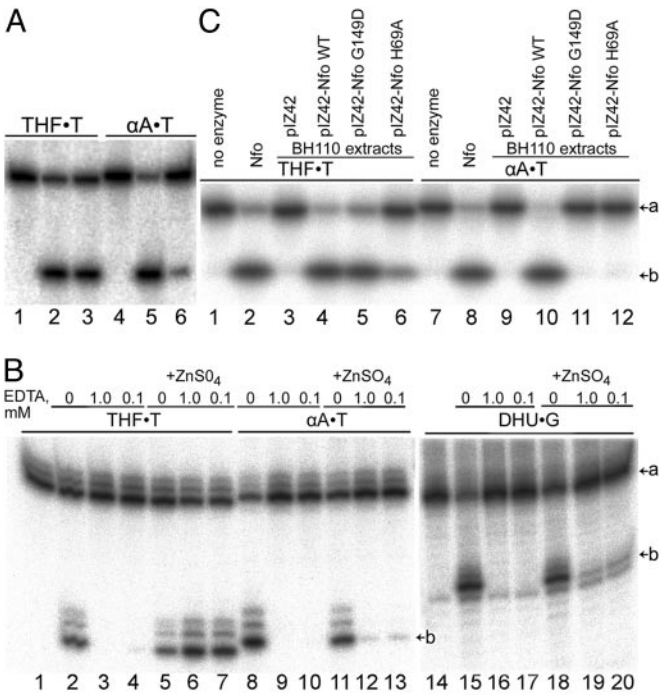


**Fig. 1.** Comparison of DNA repair activities of Nfo. (*A*) DNA repair activities of the Nfo proteins obtained from different preparations. 5′-$^{32}$P-labeled THF·T and αA·T at 5 nM were incubated with either 0.1 nM Nfo* or Nfo** for 5 min at 37°C. Lanes: 1 and 4, no enzyme; 2 and 5, Nfo*; 3 and 6, Nfo**. (*B*) Inactivation and reactivation of Nfo. 5′-$^{32}$P-labeled THF·T at 5 nM and [3′-$^{32}$P]ddAMP-labeled αA·T or DHU·G were incubated with 0.2 nM, 0.2 nM, and 1 nM Nfo, respectively, for 10 min at 37°C. Lanes: 1 and 14, no enzymes; 2–4, 8–10, and 15–17, EDTA-inactivated Nfo; 5–7, 11–13, and 18–20, EDTA-inactivated/$ZnSO_4$-reactivated Nfo. (*C*) DNA repair activities in cell-free extracts of BH110 strains harboring pIZ42 plasmids with Nfo mutants. 5′-$^{32}$P-labeled THF·T and αA·T at 5 nM were incubated with 140 ng of cell-free extracts for 5 min at 37°C. Lanes: 1 and 7, no enzyme; 2 and 8, 1 nM Nfo; 3–6 and 9–12, cell extracts. For details, see *Materials and Methods*. The letters a and b indicate substrate and cleavage product, respectively.

## Results and Discussion

**Purification Procedures and Metal Chelating Agents Alter the Substrate Specificity of Nfo.** During the course of this study, we observed strong variations in the substrate specificities of homogenous Nfo proteins obtained through two conventional purification protocols and referred here as Nfo* and Nfo**. The incision efficiency of the duplex oligonucleotide αA·T by Nfo* was ≈20-fold higher as compared with Nfo** (Fig. 1*A*, lanes 5 and 6). In contrast, both proteins exhibit similar AP endonuclease activity toward synthetic abasic site, tetrahydrofuran (THF) (Fig. 1*A*, lanes 2 and 3). Comparison of the steady-state kinetic parameters on αA·T, α-thymidine·A, DHU·G, and 5,6-dihydrothymidine·A reveals that Nfo* has 15- to 30-fold higher $k_{cat}/K_M$ values than Nfo** (Table 2, which is published as supporting information on the PNAS web site). Interestingly, the difference between the two protein preparations was mainly due to a higher turnover rate ($k_{cat}$) of Nfo*. In contrast, Nfo** had 4.7-fold higher AP endonuclease activity compared with Nfo*. These results suggest that the conventional purification procedures may change the substrate specificity of Nfo by inhibiting NIR activity.

To obtain both NIR- and AP endonuclease-proficient Nfo, we have devised a purification procedure. First, the heat treatment and ammonium sulfate precipitation steps were omitted, and all buffers used in the purification were free of metal-chelators and $Zn^{2+}$ ions. Second, a high expression level of the Nfo protein in *E. coli* BH110 (DE3) strain enabled reduction of the chromatographic steps required to obtain a homogenous protein. The newly purified Nfo protein was a more efficient AP and NIR endonuclease ($k_{cat}/K_M$, 3,100 and 1,300 $min^{-1}\cdot\mu M^{-1}$, respectively) compared with both Nfo* and Nfo**, suggesting that conventional purification techniques may indeed induce some changes in the proteins (Table 1).

The EDTA-inactivated Nfo loses intrinsic zinc atoms but can regain the AP endonuclease and 3′-repair diesterase activities by reactivation in the presence of divalent cations (5). Therefore, we hypothesized that either loss or exchange of the integral metal atom during protein purification may hamper Nfo NIR activity. To test this idea, Nfo was inactivated with 1 mM EDTA at 4°C for 48 h and then either reactivated or not in the presence or absence of 25 mM $ZnSO_4$. The reactivated enzyme samples were assayed on THF·T, αA·T, and DHU·G (Fig. 1*B*). The EDTA-inactivated Nfo completely loses the AP endonuclease (Fig. 1*B*, lanes 3 and 4) and NIR (Fig. 1*B*, lanes 9 and 10 and 16 and 17) activities. Addition of the divalent metal ions to the EDTA-treated Nfo completely restores the AP endonuclease (Fig. 1*B*, lanes 6 and 7) but not the NIR activity toward αA·T and DHU·G (Fig. 1*B*, lanes 12 and 13 and 19 and 20). These results suggest either that Nfo AP endonuclease and NIR functions have different requirements for intrinsic metal content or that the reactivated enzyme is not able to regenerate a functional NIR active site.

**Construction of the Nfo Mutants.** Previously, it was shown that a single amino acid change can modify an AP endonuclease substrate specificity, arguing that subtle alterations in the protein conformation may change its catalytic properties (16, 17). The existence of distinct Nfo isoforms obtained here suggests that DNA repair functions of the enzyme can be genetically separated. Indeed, we have shown that truncated Ape1 (NΔ61-Ape1) lacking the first 61 N-terminal amino acids has reduced NIR but normal AP endonuclease activity (3). The crystal structure of Nfo complexed to duplex DNA containing an AP site shows that three $Zn^{2+}$ ions are bound in the protein by conserved residues that cluster at the center of a crescent-shaped cavity (6). Site-directed mutagenesis of the con-

**Table 1. Steady-state kinetic parameters of the AP endonuclease, 3′-repair diesterase, and NIR activities of the WT and mutant Nfo proteins**

| | Nfo | | | Nfo-H69A | | | Nfo-G149D | | |
|---|---|---|---|---|---|---|---|---|---|
| Substrate | $K_M$, nM | $k_{cat}$, $min^{-1}$ | $k_{cat}/K_M$, $min^{-1}\cdot\mu M^{-1}$ | $K_M$, nM | $k_{cat}$, $min^{-1}$ | $k_{cat}/K_M$, $min^{-1}\cdot\mu M^{-1}$ | $K_M$, nM | $k_{cat}$, $min^{-1}$ | $k_{cat}/K_M$, $min^{-1}\cdot\mu M^{-1}$ |
| αA·T | 20 ± 2.1 | 26 ± 1.1 | 1,300 | No activity<br>28 ± 2.9† | No activity<br>0.53 ± 0.02† | No activity<br>19† | 63 ± 2.0 | 0.066 ± 0.001 | 1.0 |
| THF·T | 1.8 ± 0.3 | 5.6 ± 0.2 | 3,100 | 30 ± 2.3<br>2.1 ± 0.4† | 0.64 ± 0.02<br>0.94 ± 0.10† | 21<br>450† | 14 ± 1.6 | 19 ± 0.59 | 1,300 |
| 3′THF$^{NICK}$ | 7.5 ± 1.0 | 57 ± 1.8 | 7,500 | 16 ± 2.4 | 0.37 ± 0.02 | 23 | 91 ± 18 | 161 ± 16 | 1,800 |
| 3′p$^{NICK}$ | 6.7 ± 1.4 | 47 ± 2.5 | 6,900 | 19 ± 1.1 | 1.6 ± 0.03 | 84 | 90 ± 15 | 118 ± 12 | 1,300 |

†In the presence of 5 μM $ZnCl_2$.

served amino acid residues support participation of $Zn^{2+}$ ions in catalysis of phosphodiester bond cleavage (18). However, based on analysis of the Nfo·DNA structure and present data, we speculated that Zn1 atom, coordinated by the side chains of H69, H109, and E145, might be dispensable for cleavage of an AP site.

Here, we attempt a mutational separation of BER and NIR functions of Nfo by constructing three mutants carrying missense mutations Nfo-H69A, Nfo-H109A, and Nfo-G149D. We anticipated that H69A and H109A mutations would affect binding of the Zn1 site leading to the loss of one metal atom. As for Nfo-G149D, it was shown previously that this mutation renders cells sensitive to oxidizing agents but not to alkylating agents (17). The ability of Nfo mutant proteins to repair oxidative DNA base lesions, such as αA·T and DHU·G, was examined *in vitro*. Cell-free extracts from *E. coli nfo xth* expressing the WT and mutant Nfo proteins incised THF·T (Fig. 1*C*, lanes 4–6), indicating that all mutants contain an AP endonuclease activity. In contrast, no cleavage of αA·T was detected using Nfo-G149D and H69A mutants extracts (Fig. 1*C*, lanes 11 and 12) compared with the WT Nfo, which was fully active (Fig. 1*C*, lane 10), indicating that G149 and H69 amino acid residues are essential for NIR activity. As expected, the third mutant, Nfo-H109A, behaved similarly to the Nfo-H69A mutant (Fig. 4*A*, which is published as supporting information on the PNAS web site). Importantly, the AP endonuclease activity of Nfo-H69A (Fig. 1*C*, lane 6) and Nfo-H109A were less efficient compared with WT Nfo and Nfo-G149D (Fig. 1*C*, lanes 4 and 5). Nfo does not need metal cofactors for its activities (4), yet characterization of the purified mutant proteins reveals that the presence of $ZnCl_2$ strongly stimulates all activities of His→Ala substitution mutants but not that of G149D (Table 1 and Fig. 4*B*).

**Substrate Specificity and Metal Content of the Nfo Mutants.** All three Nfo mutant proteins were purified to homogeneity to characterize their properties. Because two His→Ala mutant proteins behaved similarly, we characterized the substrate specificities of only H69A and G149D. The $K_M$, $k_{cat}$, and $k_{cat}/K_M$ values for AP endonuclease, NIR, and 3′-repair diesterase activities using THF·T, αA·T, and duplex oligonucleotides containing THF and/or phosphate at the 3′ end of a nick were determined. In general, Nfo mutants exhibited reduced activities compared with the native Nfo on all DNA substrates tested (Table 1). We confirmed previous observation by Izumi *et al*. (17) that Nfo-G149D has 2- to 4-fold reduced 3′-repair diesterase activity than the WT Nfo. Strikingly, the $k_{cat}/K_M$ values of Nfo-G149D catalyzed NIR activity were decreased by >1,000-fold compared with WT Nfo (Table 1). In the absence of divalent cations, the Nfo-H69A mutant protein exhibited >100-fold reduced AP endonuclease and 3′-repair diesterase activities and no detectable NIR activity. Both AP endonuclease and NIR activities of the Nfo-H69A mutant protein were strongly stimulated by $ZnCl_2$ (Table 1). Similar to Nfo-G149D, the Nfo-H69A mutant exhibited more severe reduction in NIR activity as compared with AP endonuclease and 3′-repair diesterase. Interestingly, the dramatic decrease of NIR activity in both mutants was mainly due to the very low $k_{cat}$ values as compared with WT Nfo. In contrast, the moderate decrease in AP endonuclease and 3′-repair diesterase of Nfo-G149D was due to higher $K_M$ values than that of WT Nfo. Altogether, these results indicate that NIR function of Nfo can be uncoupled from AP endonuclease and 3′-repair diesterase activities.

Intrinsic metals play a critical role in the bacterial, yeast, and human AP endonucleases (3, 5). We examined the metal content of the WT and mutant Nfo proteins by using two different Zn detectors, FluoZin-3, and 4-(2-pyridylazo)resorcinol (PAR). The fluorescence emission of Zn/FluoZin-3 complexes was measured in the presence of either proteins or zinc solutions of known concentrations (Fig. 5, which is published as supporting information on the PNAS web site). The slope ratios between WT, G149D, H69A, H109, and calibration were 2.7, 1.9, 1.7, 1.6, respectively, resulting

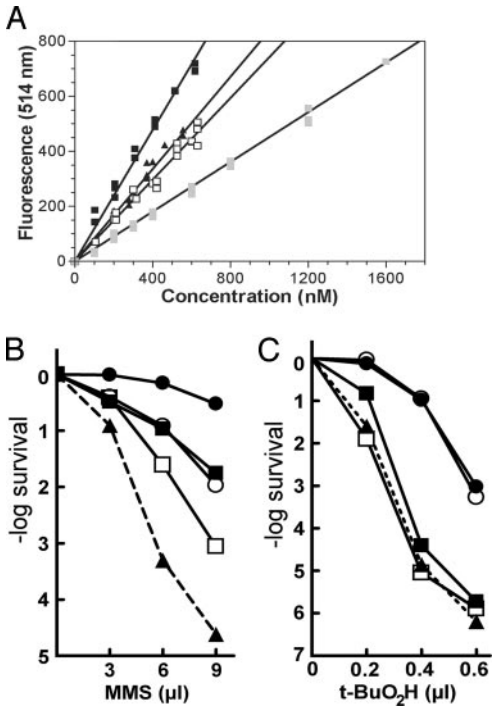


**Fig. 2.** Metal content and drug sensitivity of the Nfo mutants. (*A*) Fluorescence emission of FluoZin-3 (at 514 nm) plotted versus protein concentration of Nfo: WT (black squares), Nfo-H69A (white squares), and Nfo-G149D (black triangles). Also shown is the calibration experiment using Zn solutions of known concentrations (gray squares). (*B*) MMS sensitivity of *E. coli* AB1157 WT (black circles) and BH110 *xth nfo* strains carrying pBW21/Nfo WT (white circles), pBW21/Nfo-H69A (white squares), pBW21/Nfo-G149D (black squares), and pBR322 (black triangles). (*C*) *t*-$BuO_2H$ sensitivity of *E. coli* AB1157 WT (black circles) and BH130 *nfo* strains carrying pBW21/Nfo WT (white circles), pBW21/Nfo-H69A (white squares), pBW21/Nfo-G149D (black squares), and pBR322 (black triangles).

in stoichiometries of 2.7 atoms per WT protein, which is in agreement with previous observation (5), and only 1.9–1.6 atoms per mutant protein, suggesting that the mutants have lost approximately one $Zn^{2+}$ ion (Fig. 2*A* and data not shown). These results were confirmed by using a second method based on the absorbance at 495 nm of $(PAR)_2$-$Zn^{2+}$ complexes (Table 3, which is published as supporting information on the PNAS web site). Interestingly, the Zn content among mutants varied in the following order: Nfo-G149D > Nfo-H69A > Nfo-H109A. Indeed, lower metal content of the His→Ala mutant proteins compared with Nfo-G149D are in agreement with the role of H69 and H109 residues in the ligation of Zn1 atoms. Acquired metal-cofactor dependence of Nfo-H69A and Nfo-H109A suggests that the protein's metal-binding site fails to ligate $Zn^{2+}$ ions efficiently. Based on these results, we may propose that Zn1 is essential for Nfo-NIR function.

The reduced Zn content of Nfo-G149D is unexpected because, in contrast to His→Ala mutants, the Nfo-G149D protein does not require divalent cations and contains EDTA-resistant AP endonuclease and 3′-repair diesterase. Although the G149 residue is not directly involved in metal binding, it is located close to amino acid residue E145, which participates in the coordination of Zn1 and Zn2 atoms. Therefore, it is tempting to speculate that the negative charge and conformation of D149 residue may disturb E145-mediated coordination of Zn1. Altogether, these results suggest that (*i*) H69A, H109A, and, apparently, G149D mutations affect the ligation of a Zn atom; (*ii*) all three Zn atoms are necessary for NIR activity; and (*iii*) loss of one metal atom leads to a dramatic change in the Nfo substrate specificity. We speculate that the three Zn atoms enable Nfo to interact with

αA·T and DHU·G in a tighter manner than with an AP site and 3′-blocking group. The different mode of interaction of the enzyme generates a drastic kink of the helix DNA, which enables Nfo to access the phosphodiester bond 5′ of the damaged base. Structural studies of the enzyme/substrate complex are required to understand the mechanism of NIR catalysis.

**Differential Drug Sensitivity of *E. coli* Strains Carrying Nfo Mutations.** The AP endonuclease-deficient *E. coli nfo* and *xth* strains demonstrate differential sensitivity to oxidizing agents, such as bleomycin, *t*-$BuO_2H$, and $H_2O_2$, respectively (8, 19). The nature of specific DNA damages induced by bleomycin and *t*-$BuO_2H$, whose repair *in vivo* requires Nfo, have not yet been established. Nevertheless, it was shown that *t*-$BuO_2H$ induces in DNA single-strand breaks and oxidized sugar and bases (20), whereas bleomycin attacks successively the two DNA strands to generate complex DNA damage, such as oxidized bases, and/or AP sites closely opposed to strand breaks (21). Moreover, DNA containing these lesions is cleaved more efficiently *in vitro* by Nfo than by Xth (22). We speculate that Nfo-NIR activity is specifically required to repair this complex DNA damage *in vivo*. Availability of NIR-deficient Nfo mutants provides a tool to test this hypothesis. In the present work, we examined the methylmethanesulfonate (MMS) and *t*-$BuO_2H$ sensitivity of the AP endonuclease-deficient *E. coli* BH110 and BH130 strains harboring a plasmid with the $nfo^+$ gene. MMS, an alkylating agent, indirectly generates AP sites in DNA when methylated DNA purines are excised by DNA glycosylases (23). The *E. coli* BH110 strain lacking two AP endonucleases Xth and Nfo is extremely sensitive to both alkylating and oxidizing agents, whereas *E. coli* BH130 strain lacking Nfo is extremely sensitive to *t*-$BuO_2H$ (8). We show that the plasmids that direct the production of Nfo, Nfo-H69A, and Nfo-G149D proteins, in contrast to empty vector, conferred resistance to MMS in BH110 cells, suggesting that the Nfo mutants have the ability to repair AP sites *in vivo* (Fig. 2*B*). Consistent with biochemical data, the Nfo-H69A mutant protein, in contrast with the WT and G149D proteins, only partially restored resistance to MMS. As expected, the Nfo-H69A mutant protein did not complement at all, and the Nfo-G149D mutant protein complemented very slightly, the sensitivity of BH130 cells to *t*-$BuO_2H$ (Fig. 2*C*). Because the *E. coli* BH130 strain contains functional Xth, which provides the major AP endonuclease and 3′-repair diesterase activities, we exclude that lack of complementation of the resistance to the oxidizing agent is due to deficiency in the repair for oxidized AP sites and 3′-blocking lesions. Altogether, these results strongly argue that NIR function handles lethal oxidative DNA damage that cannot be removed in the BER pathway.

**Substrate Specificity of the Redox-Deficient Ape1 Mutant.** Because Ape1 shares common substrate specificity with bacterial Nfo, we were interested in the mutational separation of BER and NIR functions in the human enzyme. Previously, we have shown, by using a truncated NΔ61-Ape1 mutant, that the redox domain is required for NIR activity but not for AP endonuclease (3). However, it was not clear whether NΔ61-Ape1 contains 3′-repair diesterase activity. We measured activity of the NΔ61-Ape1 mutant toward 3′-blocking lesions. Under optimal conditions for NIR (pH 6.8 and 0.5 mM $MgCl_2$), NΔ61-Ape1 exhibits higher diesterase activity toward THF residues at 3′ side of a nick compared with full-length Ape1 (Fig. 6, which is published as supporting information on the PNAS web site). However, under optimal conditions for BER (pH 7.6 and 5 mM $MgCl_2$), the 3′-repair diesterase of full-length Ape1 was strongly stimulated, in contrast to NΔ61-Ape1 activity, which did not change. The fact that NΔ61-Ape1 contains proficient BER activities but deficient NIR function, similar to the Nfo mutants, suggests the existence of Ape1 NIR-deficient mutants with single amino acid changes.

AP endonucleases in living organisms have been divided into two families based on their amino acid sequence identity to either Xth or Nfo (13). Unexpectedly, Ape1 which belongs to the Xth family is involved in the NIR pathway in mammalian cells suggesting that Ape1 is in fact the mammalian functional counterpart of Nfo, rather than Xth (3). Interestingly, this evolutionary scenario parallels with eukaryotic and prokaryotic 8-oxoguanine-DNA glycosylases which belong to different enzyme families but perform same repair function (1). It is tempting to speculate that the nonconserved redox-domain of Ape1, which is absent in the prokaryotic homolog was acquired during evolution by an AP endonuclease to add NIR function to its catalytic arsenal.

**Ape1-Catalyzed NIR Activity in Cultured Human Cells.** Our goal was to formally extend our *E. coli* results to human cells. However, a direct approach is not feasible because loss-of-function studies in human cells demonstrated that Ape1 is essential for cellular viability (24, 25). Furthermore, the inhibition of Ape1 NIR activity by high $Mg^{2+}$ concentration *in vitro* raises the question of whether the intracellular environment would be compatible with this function. Therefore, to address the physiological relevance of Ape1-NIR activity in human cells, we used an approach based on the fluorescence quenching mechanism of molecular beacons (26). Because αA residues are repaired in the NIR pathway but not by DNA glycosylases (11), we constructed a single-stranded DNA oligonucleotide containing an αA residue, FD-αA, labeled with a 5′-fluorescein and a 3′-dabcyl. In the molecular beacon FD-αA, the fluorophore is held in close proximity to the quencher by the stem–loop structure design of the oligonucleotide. *In vitro*, Ape1-catalyzed incision of the beacon at αA led to separation of the fluorophore from the quencher, resulting in a continuous increase in fluorescence as a function of time (data not shown). To examine whether αA residues are repaired under intracellular conditions, the experimental FD-αA, control nondamaged FL-35 (fluorescein only), and FD-35 (fluorescein and dabcyl) beacons were transfected into HeLa and NIH 3T3 cells, and the change in fluorescence was then monitored in living cells. We observed an efficient delivery of FL-35 into cells; more importantly, during the experiment, no degradation of FD-35 occurred in NIH 3T3 cells (Fig. 7, which is published as supporting information on the PNAS web site). Consistent with the biochemical data, we observed a high fluorescence signal in the mouse cells transfected with FD-αA, implying that αA residues are recognized and cleaved efficiently by the mouse Ape1 in living cells. To further substantiate the role of Ape1 in the NIR pathway, we used RNA interference technology to suppress expression of Ape1 in HeLa cells. The efficiency of transfection of the control FL-35 beacon into HeLa cells treated or not by small inhibitory RNAs (siRNAs) was similar (approximately 30–40%). Remarkably, FD-αA-induced fluorescence was localized mainly in the nuclei of the GFP-siRNA-treated HeLa cells (Fig. 3*A*). Staining of HeLa cells with Ape1-specific antibodies showed both cytoplasmic and nuclear localization, suggesting that only the intranuclear environment is compatible with the NIR activity (Fig. 3*B*). In contrast, the cellular level of Ape1 was dramatically reduced after treatment of HeLa cells with Ape1-siRNA (Fig. 3*F*). As expected, in these cells, FD-αA induced only background fluorescence, indicating that Ape1 initiates the NIR pathway in human cells (Fig. 3*E*).

## Conclusion

The AP endonucleases Nfo, Apn1, and Ape1 are multifunctional DNA repair enzymes possessing AP endonuclease, 3′-repair diesterase, 3′→5′ exonuclease, and NIR activities. It was thought that these AP endonucleases mainly function in the BER pathway by protecting cells from abasic sites and single-strand breaks with 3′-blocking groups induced either by DNA-damaging agents or by DNA glycosylases (13, 27). Recently, we have demonstrated that AP endonuclease-initiated NIR works in concert with the BER pathway to cleanse genomic DNA of potentially mutagenic and lethal lesions (3, 28). In the present study, a genetic dissection of the BER and NIR functions of endonuclease IV reveals that the drug

BIOCHEMISTRY

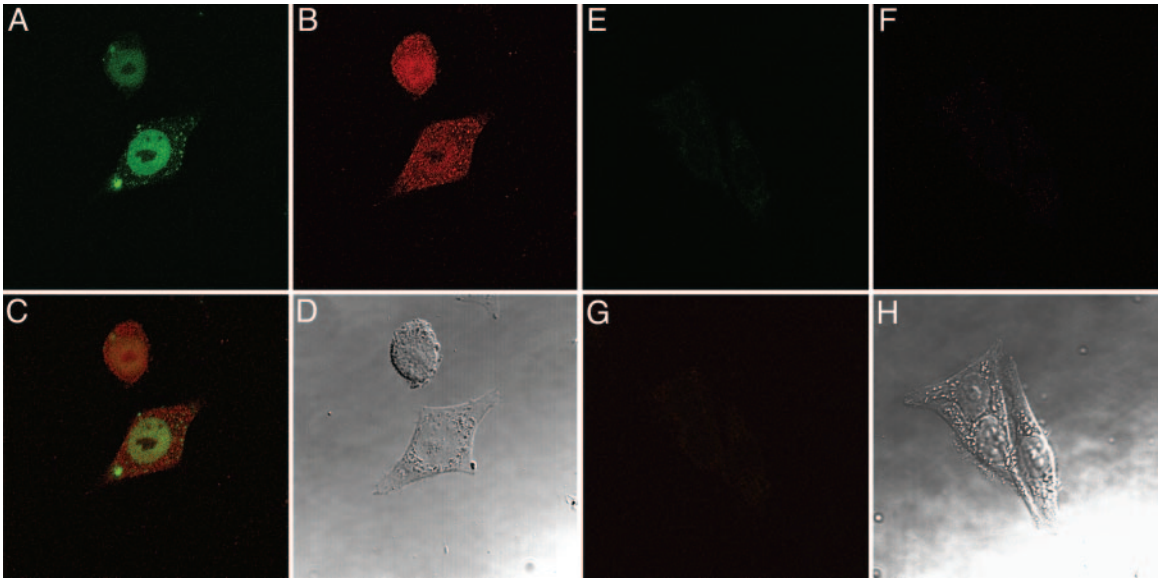


**Fig. 3.** NIR in cultured HeLa cells transfected with FD-αA. Before transfection with molecular beacon, cells were treated with either GFP-siRNA (*A–D*) or Ape1-siRNA (*E–H*). (*A* and *E*) Fluorescence. (*B* and *F*) Ape1 immunostaining. (*C* and *G*) Merge of fluorescence and Ape1 immunostaining. (*D* and *H*) Phase contrast.

sensitivity of *E. coli* correlates with the specific lack of NIR activity, thus strengthening our previous conclusions. Importantly, the compatibility of the intranuclear environment of human cells with Ape1-catalyzed NIR activity further substantiates the physiological relevance of the NIR pathway in handling oxidative DNA damage that, when left unrepaired, leads to cell death.

## Materials and Methods

**Chemicals.** MMS and *t*-$BuO_2H$ were obtained from Sigma–Aldrich and Merck–Schuchardt, respectively. The chomophoric chelator PAR and the fluorescent indicator of zinc FluoZin-3 were from Sigma–Aldrich and Molecular Probes, respectively.

**Oligonucleotides.** All oligodeoxyribonucleotides, siRNAs, and molecular beacons were purchased from Eurogentec (Seraing, Belgium), including those containing DHU, 5,6-dihydrothymidine, 5-hydroxy-2′-deoxyuridine, and THF nucleosides and 3′-terminal phosphate (3′p), 3′-terminal THF (3′THF), and complementary oligonucleotides containing dA, dG, dC, or T opposite the adduct. Oligonucleotides were end-labeled and annealed as described in ref. 3. The resulting duplex oligonucleotides are referred to as X·C (G,A,T), respectively, where X is a modified residue. The oligonucleotide and molecular beacon sequences are provided in *Supporting Materials and Methods*, which is published as supporting information on the PNAS web site.

***E. coli* Strains and Plasmids.** AB1157 (*IeuB6 thr-1 Δ(gpt-proA2) hisG4 argE3 lacY1 galK2 ara-14 mtl-1 xyl-5 thi-1 tsx-33 rpsL31 supE44 rac*) (WT) and its isogenic derivatives BH130 (*nfo*::$kan^R$) and BH110 (*nfo*::$kan^R$ [Δ(*xth-pncA)90 X*::*Tn10*]) were from the laboratory stock. The plasmids encoding the Nfo proteins, pBW21 and pIZ42, were generously provided by B. Weiss (Emory University School of Medicine, Atlanta) and T. Izumi (Louisiana State University, New Orleans), respectively.

**Sensitivity to DNA Damage Treatments.** Drug treatment was performed as described in ref. 8. Overnight bacterial cultures were diluted 100-fold in LB broth and incubated at 37°C until the optical density at 600 nm reached ≈0.6. The cells were collected by centrifugation, washed once, and suspended in PBS. Tenfold serial dilutions were prepared in PBS as well. Chemical agents MMS and *t*-$BuO_2H$ were added to 2 and 3 ml of molten LB soft agar (0.6%), respectively, at 46°C, followed immediately by 0.1–0.2 ml of each cell dilution, and the mixture was poured onto the surface of a LB agar (1.5%) plate. Colonies were scored after 2 days of incubation at 37°C on MMS-containing media and 28°C on *t*-$BuO_2H$-containing media.

**Enzyme Purifications.** In the present study, we used three different purification procedures to obtain homogenous Nfo protein. In the conventional procedure, endonuclease IV was prepared as described by Ljungquist (4) and referred to as Nfo*. In the second purification procedure, endonuclease IV was purified as described in ref. 29 and referred to as Nfo**.

In the third purification procedure, all buffers used were free of EDTA and $Zn^{2+}$, and purified endonuclease IV was referred to as Nfo. The WT and mutant Nfo proteins were overproduced in *E. coli* BH110 (DE3) and purified by using only two chromatographic steps: cells (4 g) were lysed with a French press at 18,000 psi (1 psi = 6.89 kPa) in buffer A (20 mM Hepes·KOH, pH 7.6/1 mM DTT/5% glycerol) supplemented with 500 mM NaCl and Complete protease inhibitor mixture (Roche Diagnostics). The homogenate was centrifuged at 40,000 × *g* for 20 min, and the supernatant (fraction I) was adjusted to 50 mM NaCl in buffer A and passed through a column packed with 40 ml of Q Sepharose Fast Flow (Amersham Pharmacia Biosciences, which is now GE Healthcare) preequilibrated in the same buffer. Proteins were eluted by a 50 mM NaCl–200 mM KCl gradient in buffer A. The WT and mutant Nfo proteins were eluted at the end and at the middle of the gradient, respectively. Fractions containing Nfo were pooled and diluted four times with buffer A and loaded onto a 1-ml HiTrap-Heparin column. Bound proteins were eluted in a 0.05–0.6 M KCl gradient; the WT and mutant Nfo proteins were eluted at ≈450 and 250 mM KCl, respectively. Samples of Nfo (1.5 mg/ml) were stored at −20°C in buffer containing 50% glycerol, 250 mM KCl, 40 mM Hepes·KOH (pH 7.6), and 1 mM DTT. The homogeneity of protein preparations was verified by SDS/PAGE.

**Inactivation and Reactivation of Nfo.** A solution of 10 μM Nfo in 20 mM Hepes·KOH, pH 7.6/50 mM KCl/10% glycerol/100 μg/ml BSA/0.1 mM EDTA was incubated 48 h at 4°C. For reactivation, $ZnSO_4$ was added to the final concentration of 25 mM, and the

enzyme was incubated for 1 h at 0°C. The samples were assayed as described in *Incision Assay* in the presence of 0.1 mM EDTA unless otherwise stated.

**Mutagenesis.** Site-directed mutations within the Nfo coding sequence in pBW21 and pET11a were generated by the QuikChange site-directed mutagenesis kit (Stratagene). The oligonucleotide primer sequences are provided in *Supporting Materials and Methods*. The resulting plasmids were sequenced to confirm the presence of mutations.

**Incision Assay.** The standard assay mixture for DNA-damage-specific nucleotide incision activity (20-$\mu$l final volume) contained 0.1 pmol of the 5′-[$^{32}$P]ddAMP- or 3′-[$^{32}$P]ddAMP-end-labeled oligonucleotide duplex in 20 mM Hepes·KOH, pH 7.6/50 mM KCl/1 mM DTT/100 $\mu$g/ml BSA plus limiting amounts of purified enzymes or 140 ng of cell-free extracts, unless otherwise stated. Incubations were carried out at 37°C for 10 min or for 30 min in the case of cell-free extracts, unless otherwise stated. Purified reaction products were heated at 65°C for 3 min and separated by electrophoresis in denaturing 20% (wt/vol) polyacrylamide gels [20:1, 7 M urea, 0.5× TBE (1× TBE = 90 mM Tris/90 mM boric acid/2 mM EDTA, pH 8.3)]. The gels were exposed to a Fuji FLA-3000 PhosphorScreen and analyzed with IMAGEGAUGE V3.12 software.

**Metal Content Determination.** Two different methods were used to detect zinc release from Nfo WT and mutants. The first method is based on the absorbance of light at 495 nm by the $(PAR)_2$-$Zn^{2+}$ complex (molar extinction coefficient of $6.6 \times 10^4$ $M^{-1}$·$cm^{-1}$) (30). The second method is based on the fluorescence emission of the $Zn^{2+}$/FluoZin-3 complex (31). Details of the methods are provided in *Supporting Materials and Methods*.

**DNA Repair Assay in Cultured Cells.** HeLa and NIH 3T3 cells were grown in minimum essential medium and DMEM (GIBCO), respectively, at 37°C in a humidified atmosphere with 5% $CO_2$. Culture media were supplemented with 10% of heat-inactivated FCS (GIBCO), 100 mg/ml streptomycin, and 100 unit/ml penicillin. HeLa and NIH 3T3 cells were seeded onto glass coverslips at a density of 10,000 cells per cm$^2$. Cells were washed two times with PBS, and culture medium was replaced with 1 ml of OptiMEM (Invitrogen) before transfection. Each oligonucleotide (200 pmol) and 2 $\mu$g of Cytofectin GSV (Glen Research, Sterling, VA) were diluted separately in 50 $\mu$l of solution A (100 mM NaCl/10 mM Hepes, pH 7.4) and then mixed together. After 15 min of incubation at room temperature, cytofectine/DNA complexes were added drop by drop to the cells, which were grown for 3 h and then cultured for 2 h in DMEM.

**Ape1 siRNA Knockdown Experiment.** HeLa cells were seeded onto glass coverslips at a density of 2,000 cells per cm$^2$. The next day, siRNAs complexed with Oligofectamine in OptiMEM were applied to HeLa cells to give final concentrations of 50 nM according to the manufacturer. HeLa cells were treated with either Ape1-siRNA or GFP-siRNA for 4 days. At day 4, cells were washed two times with PBS, and culture medium was replaced with 1 ml of OptiMEM. Transfection of the FD-$\alpha$A beacon was performed as described above.

**Immunostaining.** The treated cells were fixed with a 4% formaldehyde solution for 20 min at 4°C before examination in a confocal microscope (Leica SP2). The formaldehyde solution was neutralized with 50 mM $NH_4Cl$. Extraction was carried out for 4 min with 0.4% Triton X-100 in PBS. Cells were incubated for 1 h with blocking buffer (3% BSA in PBS) and then for 1 h with diluted anti-Ape1 antibodies (1/500) in blocking buffer. Cells treated with anti-Ape1 antibodies were then incubated with anti-rabbit IgG antibodies conjugated to Alexa Fluor 543 (Molecular Probes) for 30 min at room temperature. Coverslips were mounted in Vectashield (Zymed Laboratories) and observed with a confocal microscope using a plane apochromat 63 × 1.32 oil immersion objective and Leica confocal software. Alexa Fluor 543 was excited with a helium–neon ion laser (0.2 mW, 543 nm).

**Flow Cytometry Analysis.** For the flow cytometry analysis, cells were seeded on six-well plates ($2 \times 10^4$ HeLa cells). Before oligonucleotide transfection, the cells were treated by Ape1-siRNA for 4 days. At day 4, 200 pmol of FL-35 complexed to Cytofectin was incubated with the siRNA-treated and nontreated cells for 3 h and then cultured for 2 h in DMEM. Adherent cells were trypsinized and then washed with PBS. Cells were centrifuged for 10 min at 400 × *g* and resuspended in 400 $\mu$l of PBS containing 10 $\mu$g/ml propidium iodide. Mean cellular fluorescence intensities for 5,000 or 10,000 viable cells was determined on a Coulter EPICS Elite dual-laser flow cytometer. Dead cells were excluded by two means: through forward and side scatter gatings and by using propidium iodide to stain the dead cells.

We thank Drs. Jacques Laval and Andrei Kuzminov for critical reading of the manuscript, Dr. Tadahide Izumi for providing the plasmid DNA-coding Nfo-G149D mutant, Dr. Hiroshi Ide (Hiroshima University, Hiroshima, Japan) for the $\alpha$A-containing oligonucleotide, and Dr. Rhod Elder (University of Manchester, Manchester, U.K.) for Ape1 antibodies. This work was supported by European Community Grant RISC-RAD FI6R-CT-2003-508842, the Association pour la Recherche sur le Cancer, the Electricité de France Contrat Radioprotection (to M.K.S.), and a Bonus Qualité Recherche grant from the Ecole Normale Supérieure de Cachan (to E.D. and J.-C.B.). A.A.I. was supported by an Association pour la Recherche sur le Cancer Postdoctoral Fellowship.

1. Barnes, D. E. & Lindahl, T. (2004) *Annu. Rev. Genet.* **38,** 445–476.
2. Ischenko, A. A. & Saparbaev, M. K. (2002) *Nature* **415,** 183–187.
3. Gros, L., Ishchenko, A. A., Ide, H., Elder, R. H. & Saparbaev, M. K. (2004) *Nucleic Acids Res.* **32,** 73–81.
4. Ljungquist, S. (1977) *J. Biol. Chem.* **252,** 2808–2814.
5. Levin, J. D., Shapiro, R. & Demple, B. (1991) *J. Biol. Chem.* **266,** 22893–22898.
6. Hosfield, D. J., Guan, Y., Haas, B. J., Cunningham, R. P. & Tainer, J. A. (1999) *Cell* **98,** 397–408.
7. Demple, B. & Harrison, L. (1994) *Annu. Rev. Biochem.* **63,** 915–948.
8. Cunningham, R. P., Saporito, S. M., Spitzer, S. G. & Weiss, B. (1986) *J. Bacteriol.* **168,** 1120–1127.
9. Nunoshiba, T., DeRojas-Walker, T., Wishnok, J. S., Tannenbaum, S. R. & Demple, B. (1993) *Proc. Natl. Acad. Sci. USA* **90,** 9993–9997.
10. Ide, H., Tedzuka, K., Shimzu, H., Kimura, Y., Purmal, A. A., Wallace, S. S. & Kow, Y. W. (1994) *Biochemistry* **33,** 7842–7847.
11. Ishchenko, A. A., Ide, H., Ramotar, D., Nevinsky, G. & Saparbaev, M. (2004) *Biochemistry* **43,** 15210–15216.
12. Xanthoudakis, S., Miao, G., Wang, F., Pan, Y. C. & Curran, T. (1992) *EMBO J.* **11,** 3323–3335.
13. Wilson, D. M., III, & Barsky, D. (2001) *Mutat. Res.* **485,** 283–307.
14. Friedberg, E. C. & Meira, L. B. (2003) *DNA Repair* **2,** 501–530.
15. Meira, L. B., Devaraj, S., Kisby, G. E., Burns, D. K., Daniel, R. L., Hammer, R. E., Grundy, S., Jialal, I. & Friedberg, E. C. (2001) *Cancer Res.* **61,** 5552–5557.
16. Gu, L., Huang, S. M. & Sander, M. (1994) *J. Biol. Chem.* **269,** 32685–32692.
17. Izumi, T., Ishizaki, K., Ikenaga, M. & Yonei, S. (1992) *J. Bacteriol.* **174,** 7711–7716.
18. Yang, X., Tellier, P., Masson, J. Y., Vu, T. & Ramotar, D. (1999) *Biochemistry* **38,** 3615–3623.
19. Demple, B., Halbrook, J. & Linn, S. (1983) *J. Bacteriol.* **153,** 1079–1082.
20. Altman, S. A., Zastawny, T. H., Randers, L., Lin, Z., Lumpkin, J. A., Remacle, J., Dizdaroglu, M. & Rao, G. (1994) *Mutat. Res.* **306,** 35–44.
21. Povirk, L. F. (1996) *Mutat. Res.* **355,** 71–89.
22. Levin, J. D. & Demple, B. (1996) *Nucleic Acids Res.* **24,** 885–889.
23. Wyatt, M. D., Allan, J. M., Lau, A. Y., Ellenberger, T. E. & Samson, L. D. (1999) *BioEssays* **21,** 668–676.
24. Fung, H. & Demple, B. (2005) *Mol. Cell* **17,** 463–470.
25. Izumi, T., Brown, D. B., Naidu, C. V., Bhakat, K. K., Macinnes, M. A., Saito, H., Chen, D. J. & Mitra, S. (2005) *Proc. Natl. Acad. Sci. USA* **102,** 5739–5743.
26. Maksimenko, A., Ishchenko, A. A., Sanz, G., Laval, J., Elder, R. H. & Saparbaev, M. K. (2004) *Biochem. Biophys. Res. Commun.* **319,** 240–246.
27. Evans, A. R., Limp-Foster, M. & Kelley, M. R. (2000) *Mutat. Res.* **461,** 83–108.
28. Ishchenko, A. A., Yang, X., Ramotar, D. & Saparbaev, M. (2005) *Mol. Cell. Biol.* **25,** 6380–6390.
29. Ishchenko, A. A., Sanz, G., Privezentzev, C. V., Maksimenko, A. V. & Saparbaev, M. (2003) *Nucleic Acids Res.* **31,** 6344–6353.
30. Jacob, C., Maret, W. & Vallee, B. L. (1999) *Proc. Natl. Acad. Sci. USA* **96,** 1910–1914.
31. Gee, K. R., Zhou, Z. L., Qian, W. J. & Kennedy, R. (2002) *J. Am. Chem. Soc.* **124,** 776–778.